Optimization of PECVD process for ultra-thin tunnel SiO_x film as passivation layer for silicon heterojunction solar cells

Luana Mazzarella[1], Sophie Kolb[1], Simon Kirner[1], Sonya Calnan[1], Lars Korte[2], Bernd Stannowski[1], Bernd Rech[2], Rutger Schlatmann[1]

[1] PVcomB, Helmholtz-Zentrum Berlin, Berlin, 12489, Germany
[2] Institute for Silicon Photovoltaics, Helmholtz-Zentrum Berlin, Berlin, 12489, Germany

***Abstract* — Ultra-thin silicon oxide (a-SiO_x:H) films have been grown by means of plasma enhanced chemical vapor deposition (PECVD) to replace the standard hydrogenated amorphous silicon (a-Si:H) passivation layer for silicon heterojunction solar cells to reduce parasitic absorption. Additionally, silicon oxide surfaces are well known as superior substrates for the nucleation enhancement for nanocrystalline silicon doped films. Symmetrical passivation samples were fabricated with variable a-SiO_x:H layers with a thickness of 10-1.5 nm and characterized after several annealing steps (25-650 °C). The best value reached so far on <100> oriented Si wafers is: implied open circuit voltage of 686 mV and minority carrier lifetime of 1.6 ms after annealing at 300 °C. Such values were found to be reproducible even for ultra-thin a-SiO_x:H layers (1.5 nm).**

I. Introduction

Silicon heterojunction solar cells (SHJ-cells) are well known for their high efficiencies due to an excellent surface passivation which allow high circuit voltages up to 750 mV [1]. The hydrogenated amorphous silicon layers (a-Si:H) placed on the illuminated side, are responsible for parasitic absorption as the charge carriers generated therein mostly recombine instantaneously [2]. The total amount of short circuit current density (J_{sc}) lost is about 2 mA/cm^2 [2] despite the small layer thicknesses (below 10 nm). We have recently shown elswhere [3] how the J_{sc} can significantly be improved to above 40 mA/cm^2 by replacing the standard amorphous emitter with a nanocrystalline silicon oxide layer (nc-SiO_x:H).

Silicon oxide (SiO_2) can further reduce undesired parasitic absorption, when used instead of (i)a-Si:H, by acting both as passivation layer [4] and as a better substrate for enhanced nucleation in combination with nc-Si:H material, which is known to have superior optoelectronic properties compared to a-Si:H [5–8]. SiO_2 layer have to be ultra-thin (< 2 nm) to permit carrier transport by tunneling and as close as possible to stoichiometry [9].

In this paper we present a study of amorphous silicon oxide (a-SiO_x:H) growth by means of plasma enhanced chemical vapor deposition (PECVD) instead of the classical wet-chemical approch proposed by [10] in 1990 and recently by Feldmann *et al* [11] (TOPCon). The PECVD a-SiO_x film might be more challenging in terms of electrical properties and stoichiometry, but thermal annealing has been found to drastically enhance the a-SiO_x:H quality [4,12]. The a-SiO_x:H material was grown using N_2O as oxygen precursor source and deposited at low temperature. We examined the structural properties and developed a method to drastically reduce nitrogen and hydrogen incorporation in the growing film. Passivation performances were investigated for ultra-thin structures and the results indicate that a relatively low temperature annealing step (300°C) is able to improve both material and electrical quality.

II. Experimental

We fabricated a-SiO_x:H layers by PECVD with a precursor gas mixture of SiH_4, N_2O and (optionally) H_2 at a variable nitrous oxide/silane flow ratio (N_2O/SiH_4) from 0 up to 110 with the aim to grow stoichiometric SiO_2 (see Table I). The depositions were performed at a substrate temperature (T_{sub}) of 185° C at 200 Pa in an Applied Materials PECVD Cluster Tool (AKT1600) with an electrode area of ~2000 cm² by using a low power density (P_D ~15 mW/cm²) to avoid c-Si surface damage. N-type, polished c-Si float zone (270 µm, <100> oriented) wafers with a resistivity of 3 Ohm·cm were used. The wafers were cleaned by the RCA procedure and dipped in 1 % HF for 2 min prior to loading into the PECVD tool.

Layer thickness and refractive index (n) were determined by means of angle dependent spectral ellipsometry (SE) using a Sentech at incident angles between 50° and 80°. The oxide layer was modelled using the Cauchy- and the a-Si:H layer using the Tauc-Lorentz dispersion model.

Dedicated samples were fabricated by depositing a thicker a-SiO_x:H layer with a thickness of about 200 nm on one side of polished c-Si substrate to perform characterizations by Fourier transform infrared (FTIR) measurements using a Bruker Tensor 27 system. Transmission spectra were measured under nitrogen purging at room temperature with a spectral resolution of 4 cm^{-1} using 32 scans averaged per

TABLE I
PECVD Deposition Parameters

	P_D (mW/cm^2)	p (Pa)	T_{sub} (°C)	N_2O/SiH_4	SiH_4 (sccm)	H_2 (sccm)
(i)a-Si:H	20	133	190	0	300	300
a-SiO_x:H	15	200	185	17 or 35	10 or 5	900
a-SiO_x:H	15	200	185	110	4.5	/

978-1-5090-2724-8/16/$31.00 ©2016 IEEE

TABLE II
RELEVANT MOLECULAR BONDS, PEAK POSITION AND PROPORTIONALITY CONSTANT A

Molecular bond (mode)	Peak position (cm^{-1})	A [Ref.] (cm^{-2})
Si-N (str.)	970	2.07 E19 [17]
Si-O (str.)	1070	1.48 E19 [19]
Si-O (a. str.)	1100	1.48 E19 [19]
Si-H (str.)	2000-2100	9.00 E19 [15,16]
Si-H(N_3) (str.)	2300	2.00 E20 [17]
N-H (str.)	3300-3340	1.20 E20 [17]

spectrum. The measured data were corrected for atmospheric absorption using the OPUS 7 software and absorption coefficient spectra were extracted using Scout software [13]. From them it is possible to determinate the bond densities for each relevant molecular bond using experimentally proportionality constants reported in Table II.

Additionally, symmetrical samples were fabricated by coating each side with an a-SiO_x:H film (variable in thickness as specified below) capped by an a-Si:H layer, of ~15 nm thickness, to prevent further oxidation in air between deposition and the characterization procedures. (i)a-Si:H was also deposited directly onto c-Si reference sample. A Quasi-Steady-State Photoconductance lifetime (QSSPC) Sinton WCP-120 tool was used to determine the effective minority carrier lifetime (τ_{eff}) and implied open cicuit voltage (i-V_{oc}) [14]. Thermal annealing steps were performed in the Rapid Thermal Annealing (RTA) oven in a forming gas atmosphere for 30 min at several temperatures in the range 25–650 °C (ramp 150°C/min).

III A-SiO_X:H: MATERIAL CHARACTERIZATION AND OPTIMIZATION

The a-SiO_x:H films fabricated in this work were initially 10 nm thick and progressively the thickness was reduced down to 1 nm. We were able to reproduce and therefore control the passivation performances indipendently on the a-SiO_x:H layer thickness. Ellipsometry measurements confirmed a progressive reduction in refractive index with increasing the N_2O/SiH_4 ratio in the gas phase as reported in Fig. 1 (b). For the film deposited with the highest diluted condition (N_2O/SiH_4=110), the refractive index measured was very close to the stoichiometry (n= 1.47, curve d.).

The a-SiO_x:H layers were characterized by means of FTIR with the aim of controlling stoichiometry, material quality and annealing effect. Dedicated samples were deposited on c-Si substrates by varying the oxygen content (N_2O/SiH_4 ratio in Table I)). The absorption coefficient spectra were measured in the as-grown condition (depicted in Fig. 1 (a)) and after annealing treatment at 300 and 650 °C. Moreover, the relevant molecular bonds and vibration modes were identified as reported previously in Table II. The intrinsic amorphous reference layer shows the vibrational modes of Si–Si and Si–H bonds in corresponding to peaks centered at 600 cm^{-1} and 2000-2100 cm^{-1}, respectively (Fig. 1, curve a.). The Si-H broad peak is a distinctive indication of the hydrogen content within the layer [15,16], which is reduced after annealing at 300 °C and entirely disappeared after a high temperature treatment (650°C) (not shown here). The absorption coefficient spectra of a-SiO_x:H films are plotted in the same Fig. 1 (a) for a variable N_2O/SiH_4 ratio, we extracted interesting information. The layer deposited with lower N_2O flow and strongly diluted in H_2 (Table I) is rather a silicon-oxide-nitride (a-SiO_xN_y:H) material (curve b.). The peaks caused by Si-N and N-H stretching modes are identified at 870 cm^{-1} and at 3390 cm^{-1}, additionally the Si-H stretching regime is shifted to higher frequencies from a-Si:H to a-SiO_xN_y:H due to the presence of N [17] (2250 cm^{-1} in Fig. 1 (a)). The dissociation analysis of the N_2O molecules in a discharge plasma performed by Date *et al.* [18] reveals that NO and N can be minor dissociated products besides the more abundant N_2 and O_2. Also, Pai *et al.* [19] have shown that N impurities and Si-H and N-H bonding groups that could be removed by adding He to the PECVD gas mixture. We partially lowered the incorporation of the undesired species by (1) increasing the N_2O flow and (2) removing the H_2 from the precursor mixture. Curve c. in Fig. 1 (a) shows the effect of the higher N_2O/SiH_4 ratio on the growing film that considerably reduced both Si-N and N-H modes. No shifted Si-H peak is detectable. Moreover, the peak associated with the Si-O stretching mode shifts towards higher wavenumbers, which is an indication of the approach the stoichiometry.

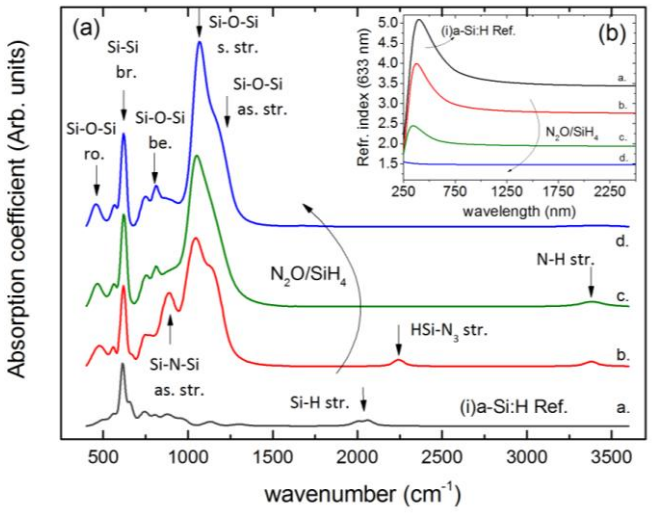

Fig. 1. (a) Absorption coefficient as function of wavenumber of (i)a-Si:H and a-SiO_x:H films measured at room temperature in the as-grown condition. The N_2O/SiH_4 ratios for the curves b. c. and d. are 17, 35 and 110. Bonding and mode are identified for the relevant peaks (ro.=rocking, be.=bending, br.=breathing, str.=stretching, as.=asymmetric, s. =symmetric). The curves are vertically shifted for clarity. (b) Refractive index spectra as function of wavelength measured by ellipsometry for the same a-SiO_x:H films and (i)a-Si:H reference.

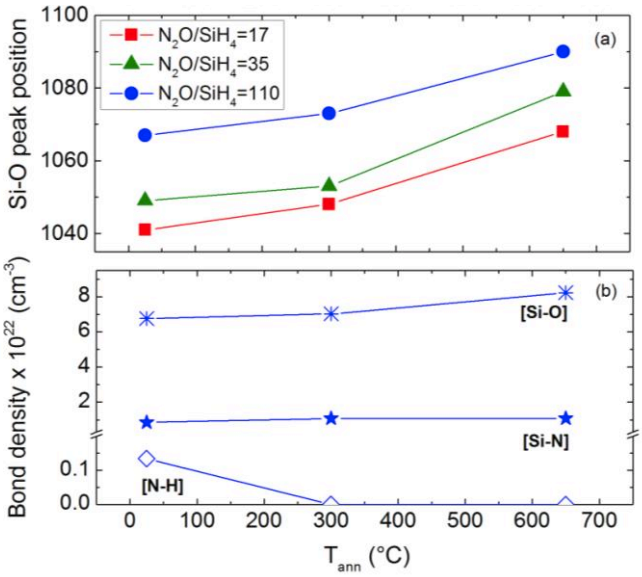

Fig. 2. (a) Evolution of the Si-O peak position as function of the annealing temperatures. (b) Densities of Si-O, Si-N and N-H bonds for the more stoichiometric film. Lines are guides for the eyes.

Finally, the film deposited with a further increased N_2O and without hydrogen flow (curve d.) shows a typical SiO_2 spectrum with the characteristic Si-O regimes at 470, 830 1070 and the shoulder at 1120 cm^{-1}, corresponding to the Si-O rocking, bending, symmetrical and asymmetrical stretching mode, respectively (Fig. 1 (a))) [19]. The heavy reduction of the SiH_4 and the lack of the additional source of H into the deposition environment was believed to lower the possible interactions of NO and N species. This might explain the very low amount of both nitrogen and hydrogen in our optimized layer. Only a broad and very low intensity N-H peak (not visible in curve d.) was measured. The resulting material is close to the stoichiometry, which is also indicated by ellipsometry.

The thermal annealing improves the film quality due to an increase in the structural order and/or induced thermal relaxation of the lattice. One of the principal effects is the shift of the Si-O peak position to higher wavenumbers [12] as shown in Fig. 2 (a). Calculated bond densities for the more stoichiometric layer are plotted in Fig. 2 (b) as function of the annealing temperature. The most noticeable consequence of the thermal exposure concerns the weak N-H peak at 3390 cm^{-1} that vanishes at T_{ann} of 300°C. The reason for the increased Si-O density after each annealing step is surface oxidation.

IV A-SiO$_x$:H: PASSIVATION PERFORMANCE

The a-SiO_x:H films were further investigated as passivation layers for application in SHJ solar cells. Fig. 3 shows the evolution of the i-V_{oc} for symmetrical samples with a-SiO_x:H (variable)/(i)capping layer (15 nm) stack on each wafer side as function of the annealing temperature in forming gas (FG). Considering the as-deposited values measured at room temperature (25 °C) we see that the (i)a-Si:H reference gives the best passivation, and i-V_{oc} decreases rapidly with increasing the oxygen content, as also found in [20]. As mentioned before, the a-SiO_x:H layer needs to be annealed and for this purpose we thermally treated the samples in an RTA oven (in forming gas). Carrier lifetimes were measured after each annealing step (Fig. 3). The (i)a-Si:H reference improved with annealing up to 250 °C, which can be explained by hydrogen diffusion to the a-Si:H/c-Si interface and passivation of dangling bonds. At higher temperature the (i)a-Si:H films degraded due to hydrogen effusion out of the layer [21], that was also confermed by FTIR (not shown here).

The a-SiO_x:H samples in Fig. 3 show a higher thermal stability than the silicon amorphous one with a pronunced improvement in i-V_{oc} (+ above 160 mV) and a maximum at T_{ann} = 300 °C. The maximum values of i-V_{oc} = 686 mV and τ_{eff} = 1.6 ms were achieved for the highest N_2O/SiH_4 ratio, that is consistent with the highest stoichiometry ratio demostrated in the paragraph III. For the lower oxygen content sample the i-V_{oc} is limited up to 660 mV probably caused by the relevant nitrogen content. At higher temperatures, the passivation reverted to the as-deposited values. The lifetime curves measured for the sample with better perfomances (N_2O/SiH_4=110) after each annealing step are plotted in Fig. 4. They give further information about the dominant recombination mechanisms [22]. The strong increase in τ_{eff} after the 300°C can be explained by a stronger field effect via accumulation of a positive fixed charge at the silicon interface which is progressively reduced at higher annealing temperatures. Considering the structural investigation discussed in section III, the vanishing of weakly bonded N atoms might also play a role in the improved electrical

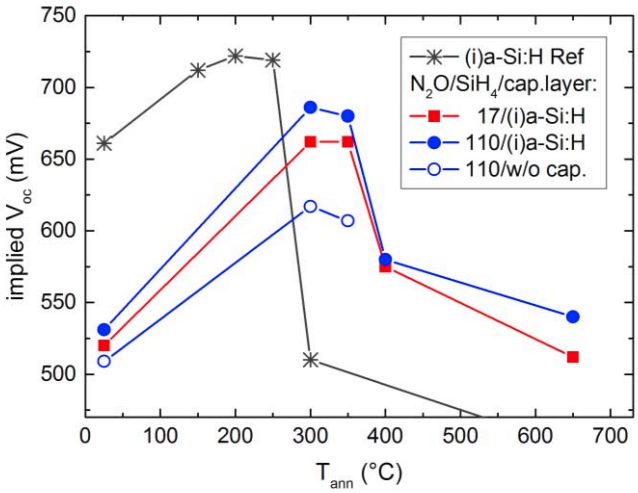

Fig. 3. Implied V_{oc} as a function of annealing temperature of a-SiO_x:H symmetric samples with varying the N_2O/SiH_4 ratio from 17 (blue points) to 110 (red points). The a-SiO_x:H film is 1.5 nm thick,. The (i)a-Si:H sample with a layer thickness of 15 nm was added as a reference.

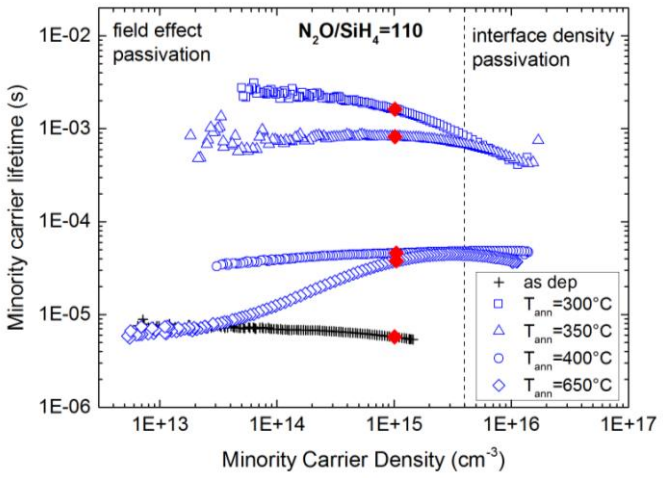

Fig. 4. Minority carrier lifetime as a function of minority carrier density for different annealing temperatures. The sample is the same reported in Fig. 3 for N_2O/SiH_4=110 and capping layer.

properties. A symmetric sample coverd only with a thicker a-SiO_x:H (10 nm) was also fabricated with the aim of separating the effect of the FG from the capping layer one. This sample proves that the specific gas atmosphere is required [4,23] but also that the capping layer plays a role in improving the passivation performances. We hypothesize that the H atoms present into the (i)a-Si:H network can diffuse, thanks to the temperature and the FG atmosphere, towards the a-SiO_x:H film. Contrary to the findings of Ding *et al.* [23], the deposition of p- or n-doped nc-Si materials does not increase the lifetime in the as-grown condition (not shown here).

V Conclusions

In this work, we optimized the PECVD of an ultra-thin a-SiO_x:H film for use as a tunnel oxide in SHJ solar cells. A higher dilution of SiH_4 in N_2O mixture and the omission of H_2 from the gas phase, were found to be critical for growing stoichiometric layers (n= 1.47) with drastically reduced nitrogen and hydrogen content (Fig. 1 and 2). The layer thickness was also successfully reduced down to 1 nm while maintaining passivating properties. As expected, the optimized a-SiO_x:H shows low passivation performances in the as-grown condition that were overcome by a subsequent thermal treatment in FG. At relatively low annealing temperature (300 °C) the carrier lifetime was enhanced up to 1.6 ms (in Fig. 3) for the a-SiO_x:H film due to induced relaxation/order in the lattice and improved stoichiometry, as demonstrated by FTIR analysis. Further experiments under development aim to combine the oxidic ultra-thin buffer with nc-Si:H doped films. Early stage results have demonstrated a superior nanocrystalline evolution and reduction in parasitic absorption that makes the stack attractive for window applications in SHJ solar cells.

Acknowledgement

The authors thank K. Bhatti, M. Hartig, T. Hänel, T. Henschel, K. Jacob, K. Mack and M. Wittig for technical support. This work was partially supported by the European Commission through the FP7-ENERGY project "HERCULES" (Grant No. 608498).

References

[1] M. Taguchi, A. Yano, S. Tohoda, K. Matsuyama, Y. Nakamura, T. Nishiwaki, K. Fujita and E. Maruyama,"24.7% Record Efficiency HIT Solar Cell on Thin Silicon Wafer", *IEEE Journal of Photovoltaics*, vol. 4, pp. 96–99, 2014.

[2] Z. Holman, A. Descoeudres, L. Barraud, F. Fernandez, J. Seif, S. de Wolf and C. Ballif,"Current Losses at the Front of Silicon Heterojunction Solar Cells", *IEEE Journal of Photovoltaics*, vol. 2, pp. 7–15, 2012.

[3] L. Mazzarella, S. Kirner, B. Stannowski, L. Korte, B. Rech and R. Schlatmann,"p-type microcrystalline silicon oxide emitter for silicon heterojunction solar cells allowing current densities above 40 mA/cm2", *Applied Physics Letters*, vol. 106, p. 23902, 2015.

[4] Z. Chen, S. Pang, K. Yasutake and A. Rohatgi,"Plasma-enhanced chemical-vapor-deposited oxide for low surface recombination velocity and high effective lifetime in silicon", *Journal of Applied Physics*, vol. 74, p. 2856, 1993.

[5] P. Roca i Cabarrocas, N. Layadi, T. Heitz, B. Drévillon and I. Solomon,"Substrate selectivity in the formation of microcrystalline silicon: Mechanisms and technological consequences", *Applied Physics Letters*, vol. 66, p. 3609, 1995.

[6] E. Vallat-Sauvain, J. Bailat, J. Meier, X. Niquille, U. Kroll and A. Shah,"Influence of the substrate's surface morphology and chemical nature on the nucleation and growth of microcrystalline silicon", *Thin Solid Films*, vol. 485, pp. 77–81, 2005.

[7] M. Bailly, J. Carpenter, Z. Holman and S. Bowden,"Substrate dependent growth of microcrystalline silicon", *IEEE Journal of Photovoltaics*, pp. 1201–1205, 2014.

[8] M. Tzolov, F. Finger, R. Carius and P. Hapke,"Optical and transport studies on thin microcrystalline silicon films prepared by very high frequency glow discharge for solar cell applications", *Journal of Applied Physics*, vol. 81, p. 7376, 1997.

[9] A. Moldovan, F. Feldmann, M. Zimmer, J. Rentsch, J. Benick and M. Hermle,"Tunnel oxide passivated carrier-selective contacts based on ultra-thin SiO2 layers", *Solar Energy Materials and Solar Cells*, vol. 142, pp. 123–127, 2015.

[10] K. Kawabata, H. Morikawa, T. Ishihara, K. Sato, H. Sasaki, T. Itagaki, M. Deguchi, S. Hamamoto and M. Aiga,"Formation of PN junction with hydrogenated microcrystalline silicon", Kissimmee, FL, USA, 21-25 May 1990, pp. 659–663

[11] F. Feldmann, M. Simon, M. Bivour, C. Reichel, M. Hermle and S. Glunz,"Efficient carrier-selective p- and n-contacts for Si solar cells", *Solar Energy Materials and Solar Cells*, vol. 131, pp. 100–104, 2014.

[12] E. San Andrés, A. del Prado, I. Mártil, G. González-Díaz, D. Bravo and F. López,"Thermally induced modifications on bonding configuration and density of defects of plasma deposited SiO[sub x]: H films", *Journal of Applied Physics*, vol. 92, p. 1906, 2002.

[13] Theiss, W. Scout "*Tutorial* 1", 2012, http://www.wtheiss.com/docs/scout_tutorial1.pdf.

[14] R. Sinton and A. Cuevas,"Contactless determination of current–voltage characteristics and minority-carrier lifetimes in semiconductors from quasi-steady-state photoconductance data", *Applied Physics Letters*, vol. 69, p. 2510, 1996.
[15] H. Shanks, F. Jeffrey and M. Lowry,"Bonding in hydrogenated amorphous silicon", *Le Journal de Physique Colloques*, vol. 42, pp. C4-773-C4-777, 1981.
[16] A. Langford, M. Fleet, B. Nelson, W. Lanford and N. Maley,"Infrared absorption strength and hydrogen content of hydrogenated amorphous silicon", *Physical Review B*, vol. 45, pp. 13367–13377, 1992.
[17] E. Bustarret, M. Bensouda, M. Habrard, J. Bruyère, S. Poulin and S. Gujrathi,"Configurational statistics in a - SixNyHz alloys: A quantitative bonding analysis", *Physical Review B*, vol. 38, pp. 8171–8184, 1988.
[18] L. Date, K. Radouane, B. Despax, M. Yousfi, H. Caquineau and A. Hennad,"Analysis of the N 2 O dissociation in a RF discharge reactor", Journal of Physics D: *Applied Physics*, vol. 32, pp. 1478–1488, 1999.
[19] P. Pai,"Infrared spectroscopic study of SiOx films produced by plasma enhanced chemical vapor deposition", *Journal of Vacuum Science & Technology A: Vacuum, Surfaces, and Films*, vol. 4, p. 689, 1986.
[20] M. Mews, M. Liebhaber, B. Rech and L. Korte,"Valence band alignment and hole transport in amorphous/crystalline silicon heterojunction solar cells", *Applied Physics Letters*, vol. 107, p. 13902, 2015.
[21] J. Schüttauf, C. van der Werf, I. Kielen, W. van Sark, J. Rath and R. Schropp,"Improving the performance of amorphous and crystalline silicon heterojunction solar cells by monitoring surface passivation", *Journal of Non-Crystalline Solids*, vol. 358, pp. 2245–2248, 2012.
[22] A. Cuevas and D. Macdonald,"Measuring and interpreting the lifetime of silicon wafers", *Solar Energy*, 76, pp. 255–262, 2004.
[23] K. Ding, M. Pomaska, A. Singh, F. Lentz, F. Finger and U. Rau,"Mechanism for crystalline Si surface passivation by the combination of SiO 2 tunnel oxide and μc-SiC: H thin film", *Physica Status Solidi (RRL) - Rapid Research Letters*, vol. 10, pp. 233–236, 2016.